Vol 14 No 9, September 2005
1009-1963/2005/14(09)/1879-03

Chinese Physics

Magnetotransport properties of $La_{0.67}Ca_{0.33}MnO_3/La_{0.67}Sr_{0.33}MnO_3$ bilayers*

Feng Jia-Feng(丰家峰)[a], Zhao Kun(赵 昆)[a,b,c†], Huang Yan-Hong(黄延红)[a], Zhao Jian-Gao(赵见高)[a], Han Xiu-Feng(韩秀峰)[a], Zhan Wen-Shan(詹文山)[a], and Wong Hong-Kuen(黄康权)[d]

[a] *Beijing National Laboratory for Condensed Matter Physics, Institute of Physics, Chinese Academy of Sciences, Beijing 100080, China*

[b] *Spintronics Laboratory, School of Physics Science and Information Technology, Liaocheng University, Liaocheng 252059, China*

[c] *International Center for Materials Physics, Chinese Academy of Sciences, Shenyang 110016, China*

[d] *Department of Physics, The Chinese University of Hong Kong, Hong Kong*

(Received 31 March 2005; revised manuscript received 21 April 2005)

The perovskite bilayers $La_{0.67}Ca_{0.33}MnO_3$ (LCMO) (100 nm) / $La_{0.67}Sr_{0.33}MnO_3$(LSMO) (100 nm) and LSMO (100 nm) / LCMO (100 nm) are fabricated by a facing-target sputtering technique. Their transport and magnetic properties are investigated. It is found that the transport properties between them are different obviously due to distinguishable structures, and the different lattice strains in both films result in the difference of metal-to-insulator transition. Only single-step magnetization loop appears in our bilayers from 5K to 320K, and the coercive force of LSMO/LCMO varies irregularly with a minimum $\sim$ 2387A/m which is lower than that of LCMO and LSMO single layer films. The behaviour is explained by some magnetic coupling.

Keywords: manganites, magnetic coupling, bilayer film
PACC: 7130, 7500, 7570

1. Introduction

The doped manganites, $RE_{1-x}A_xMnO_3$ (RE = rare-earth and A = alkaline-earth elements), have been the topic of intense scrutiny in recent years because of displaying a fascinating diversity of behaviour including several forms of magnetic, orbital and charge orderings as well as the colossal magnetoresistance (CMR) near the ferromagnetic Curie temperature (T_C).[1−5] Another distinguishing feature is that the spin polarization in the doped manganites is believed to be 100% due to the half-metallic nature, where only the single spin band crosses the Fermi level.[6] Because of the high spin polarization of conduction electrons in the doped manganites, spin-polarized tunnel junctions or other devices with the doped manganites as ferromagnetic layers (FMs) show high low-field magnetoresistance (MR).[7] It is argued that the high MR originates from the magnetic coupling at the interface. However, their contact with antiferromagnetic (AF) perovskite layers and substrates may give rise to some divertive effects, which may alter the magnetotransport and magnetic properties of the devices, if the doped manganites serve as FMs. Therefore, to optimize extrinsic MR effects in manganite-based devices, it would be necessary to have a full understanding of interlayer magnetic interactions and of substrate-induced effects in the magnetic and transport properties, although a full understanding of them still remains open.

In this paper, we have a systemic study of the magnetic properties of $La_{0.67}Ca_{0.33}MnO_3$ (LCMO) / $La_{0.67}Sr_{0.33}MnO_3$ (LSMO) and LSMO/LCMO bilayers. It is considered that these two compounds have similar lattice parameters, which make them very attractive to form heterostructures with good interfaces.

*Project supported by the National Natural Science Foundation of China (Grant Nos 50371102 and 10334070), Hi-Tech Research and Development Program of China (Grant No 2004AA32G090), the Research Foundation of Shandong Provincial Education Department of China (Grant No 03A05), the Hong Kong Research Grant Council, and China Postdoctoral Science Foundation.

†E-mail: kzhao@aphy.iphy.ac.cn

The metal-to-insulator transition temperature, $T_{\rm mi} \approx$ 240K, of bulk LCMO is much lower than the metal-to-metal transition temperature, $T_{\rm mm} \approx$365K, of bulk LSMO. In our setup, there is a rather broad temperature range within which the LCMO is paramagnetic and insulator, whereas the LSMO is ferromagnetic and metallic.

2. Experimental procedures

LSMO (100 nm) / LCMO (100 nm) and LCMO (100 nm) / LSMO (100 nm) bilayers were prepared on (110) $NdGaO_3$ (NGO) single-crystal substrates at 680°C by a facing-target sputtering technique from stoichiometric ceramic LCMO and LSMO targets,[8−12] which were sintered by standard procedure. The structure of the samples was analysed by a Huber four-circle x-ray diffractometer using Cu Kα x-rays. The resistance, R, as a function of temperature was carried out by using the standard four-probe method. The magnetic hysteresis loop of the samples was measured by utilizing a vibrating sample magnetometer between 5 and 300K, and by applying an magnetic field parallel to the sample surface. A small nonhysteretic contribution from the NGO substrate was eliminated by separately measuring its diamagnetic response.

3. Results and discussion

X-ray diffraction (XRD) study shows that both bilayers are good epitaxial films, and only those peaks which are coherent with the substrate were detected. Figure 1 shows the XRD patterns of the as-prepared LCMO (100 nm) / LSMO (100 nm) / NGO and LSMO (100 nm) / LCMO (100 nm) / NGO. The reflections of Cu Kα_1 and Kα_2 can be distinguished from each other. Taking the diffraction peaks for the substrate as an internal standard, we can determine accurately the out-of-plane lattice parameters of LCMO and LSMO layers, $d_{\rm LC}$ and $d_{\rm LS}$. As for LSMO/LCMO/NGO, $d_{\rm LC}$=0.7770nm and $d_{\rm LS}$=0.7808nm, while $d_{\rm LC}$ = 0.7767nm and $d_{\rm LS}$=0.7814nm for LCMO/LSMO/NGO.

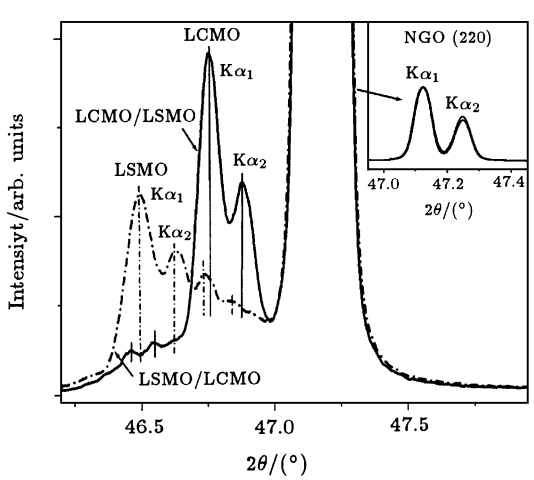

Fig.1. X-ray diffraction patterns of LCMO (100nm) / LSMO (100nm) / NGO and LSMO (100nm) / LCMO (100nm) /NGO. The inset is a close view of the (220) peak of the NGO substrate.

For thin epitaxial film, the in-plane lattice of the sample has to match that of the substrate, and then the lattice expansion is essentially the expansion of the out-of-plane lattice parameter. LSMO has larger lattice parameters than that of LCMO, whereas NGO exhibits negligibly smaller lattice constants than LCMO. A tensile strain in LSMO–NGO and LSMO–LCMO and a small lattice strain in LCMO–NGO should be expected. Therefore, the out-of plane lattice of LCMO and LSMO layer should be stress and expansion, respectively. Different from the cap LSMO layer in LSMO/LCMO/NGO, the middle LSMO layer in LCMO/LSMO/NGO is stressed by NGO substrate and LCMO layer, which indicates the larger value of $d_{\rm LS}$. In the same way, the difference between the $d_{\rm LC}$ can be also understood easily. Compared with the cap LCMO layer in LCMO/LSMO/NGO, the middle one in LSMO/LCMO/NGO is not only expanded by LSMO layer but also stressed slightly by NGO substrate, which results in the larger $d_{\rm LC}$.

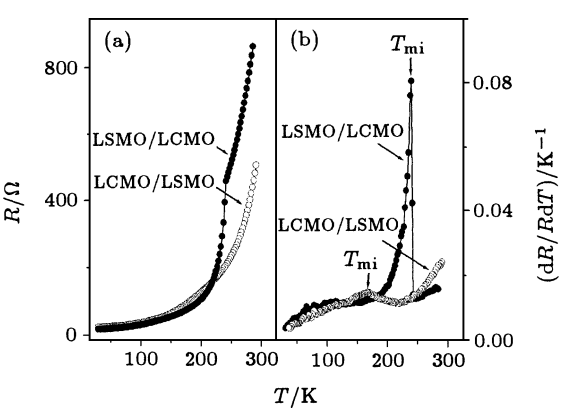

Fig.2. (a) Resistance (R) and (b) differential coefficient (dR/RdT) as functions of temperature for bilayer films, LCMO (100nm) / LSMO (100nm) / NGO and LSMO (100nm) / LCMO (100 nm) / NGO, respectively.

Figures 2(a) and 2(b) show the temperature dependence of the resistance (R) and its temperature coefficient (dR/RdT) of bilayers. The two samples are all metallic conductions in the entire temperature range investigated. As for LSMO/LCMO/NGO, the resistance decreases smoothly with cooling at first,

subsequently a very visible jump happens in the vicinity of 240 K, and results in a peak value for dR/RdT. In fact, this transition is in good agreement with the metal–insulator transition of LCMO (100nm) / NGO single layer film. So we also denote the transition temperature as T_{mi}. Very different from that in LSMO/LCMO, the metal-to-insulator transition resulted from LCMO layer in LCMO/LSMO is not sharp and shifts to lower temperature, $T_{mi} \sim 166$K. Based on our XRD data of powder samples, the lattice mismatch of (110) plane is 0.8% and 0.03% for LCMO–LSMO and LCMO–NGO, respectively. The different lattice strains in both films are responsible for the different T_{mi}.

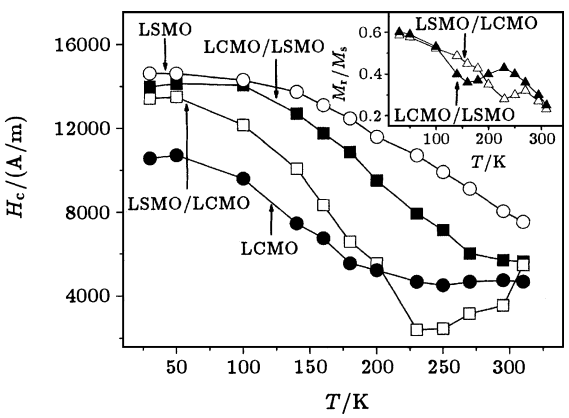

Fig.3. H_c as a function of temperature for LCMO (100 nm) / NGO (●), LSMO (100nm) / NGO (○), LCMO (100nm) / LSMO (100nm) / NGO (■) and LSMO (100 nm) / LCMO (100 nm) / NGO (□) films, respectively. The inset shows the temperature dependence of M_r/M_s for LCMO (100nm) / LSMO (100nm) / NGO and LSMO (100nm) / LCMO (100nm) / NGO bilayers.

Figure 3 is a summary of magnetic coercivity H_c against the temperature. In addition, we obtain the rest magnetization M_r versus M_s ratio, M_r/M_s, for both the bilayers in the temperature range investigated (see the inset in Fig.3). The local minimum in the M_r/M_s curve occurs at the vicinity of T_{mi}, and is consistent with the metal-to-insulator transition of LCMO layers. As for LCMO (100nm) / NGO and LSMO (100nm) / NGO single layer films, their coercivities are distinct obviously in the whole temperature range. In general, alternating hard and soft magnetic phases can lead to either a broad or a narrow waist loop. Arising from the different coercivities between LCMO and LSMO layers, a two-step loop should have been measured if the systems were decoupled. In fact, only single-step magnetization loop appears in our bilayers from 5K to 320K, indicating that there is some magnetic coupling in the systems. The coercive force basically reduces monotonously with increasing temperature of LCMO/LSMO bilayer, while the H_c of LSMO/LCMO varies irregularly and has a minimum ~ 2387A/m at ~ 230K. In special, the value of H_c is lower than that of LCMO and LSMO single layer films in the range between 200K and 300K. It is quite reasonable that the exchange coupling between LSMO and LCMO layers brings on the nonmonotonic H_c. The different trends of H_c between the two bilayers suggest that different coupling modes rule over, which may be resulted from the different lattice distortion. It is argued that these results originate from the inter-layer magnetic interaction, although a full understanding of the effects still remains open.

4. Conclusion

In summary, we performed a structure and magnetotransport characterization of LSMO/LCMO and LCMO/LSMO bilayers. The transport properties between them are different obviously due to distinguishable structures, and the different lattice strains in both films result in the different T_{mi} of LCMO layers. The different trends of H_c between the two bilayers suggest that some magnetic coupling modes rule over, which may result from the lattice distortion.

References

[1] Von Helmolt R, Wecker J, Holzapfel B, Schultz L and Samwer K 1993 *Phys. Rev. Lett.* **71** 2331
[2] Jin S, Tiefel T H, McCormack M, Fastnacht R A, Ramesh R and Chen L H 1994 *Science* **264** 413
[3] Xiao C T, Han L A, Xue D S and Zhao J H 2003 *Acta Phys. Sin.* **52** 1245
[4] Duan P, Tan G T, Dai S Y, Chen Z H, Zhou Y L and Lü H B 2003 *Acta Phys. Sin.* **52** 2061
[5] Lu Y, Li Q A, Di N L, Li R W and Cheng Z H 2003 *Chin. Phys.* **12** 1301
[6] Park J H, Vescovo E, Kim H J, Kwon C, Ramesh R and Venkatesan T 1998 *Nature* **392** 794
[7] Obata T, Manako T, Shimakawa Y and Kubo Y 1999 *Appl. Phys. Lett.* **74** 290
[8] Zhao K, Zhou L Z, Leung C H, Yeung C F, Fung C K and Wong H K 2002 *J. Cryst. Growth* **237–239** 608
[9] Zhao K and Wong H K 2003 *J. Cryst. Growth* **256** 283
[10] Zhao K and Wong H K 2004 *Physica* B **349** 238
[11] Zhao K and Wong H K 2004 *Physica* C **403** 119
[12] Zhao K, Zhang L, Li H and Wong H K 2004 *J. Appl. Phys.* **95** 7363